Int J Adv Manuf Technol (2012) 63:415–420
DOI 10.1007/s00170-012-3921-x

ORIGINAL ARTICLE

Effects of electromagnetic stirring and rare earth compounds on the microstructure and mechanical properties of hypereutectic Al–Si alloys

Prabhkiran Kaur · D. K. Dwivedi · P. M. Pathak

Received: 11 March 2011 / Accepted: 10 January 2012 / Published online: 25 January 2012

Abstract In this paper, the effects of rare earth addition and electromagnetic stirring on the microstructure and the mechanical properties of hypereutectic Al–Si alloys have been reported. Hypereutectic Al–Si alloy was prepared using liquid metallurgy route and modified with the addition of cerium oxide. To control the structure, slurry of hypereutectic Al–Si alloy was subjected to electromagnetic stirring before pouring into the mould. It was observed that the addition of cerium oxide (0.2 wt.%) refined the primary silicon particles and modified the eutectic silicon particles. Further, the electromagnetic stirring of the hypereutectic Al–Si alloy reduced the average size of primary silicon particles, from 152±9 to 120±6 μm, and the length of β-intermetallic compounds decreased from 314±12 to 234±10 μm. Similarly, the application of electromagnetic stirring on cerium oxide-modified hypereutectic Al–Si alloy also reduced the average size of primary silicon particles from 98±5 to 76±4 μm and the average length of β-intermetallic compounds from 225±7 to 203±5 μm. Mechanical properties namely tensile strength, ductility and hardness of the alloys were improved with electromagnetic stirring and addition of cerium oxide appreciably.

Keywords Hypereutectic Al–Si alloy · Electromagnetic stirring · Microstructure · Mechanical properties

1 Introduction

The hypereutectic Al–Si alloys are used for manufacturing a variety of tribological and automotive components owing to good wear resistance and fair strength-to-weight ratio. The mechanical and tribological performances of these alloys are primarily governed by morphology of the primary silicon particle and that of eutectic matrix. Large cuboid-shaped primary silicon particles are known to deteriorate mechanical and tribological properties of hypereutectic Al–Si alloys besides lowering of the machinability; therefore, refinement of primary silicon particles becomes mandatory to produce acceptable castings [1, 2]. Traditionally, phosphorous (P)-based compounds have been used for refining the primary silicon particles; however, this method suffers with high volatility of P. Therefore, attempts are being made to explore new methods for refining the primary silicon particle (PSP) of these alloys. Semi-solid metal processing has been reported to spheroidize and refine the alpha aluminium grains but not many studies have been reported on the application of semi-solid processing of hypereutectic Al–Si alloys using electromagnetic stirring approach [2, 3]. Recently, many studies have been published on the influence of rare earth (RE) elements such as lanthanum and cerium on the structure and properties of hypereutectic Al–Si alloys [4–9]. It has been reported that cerium (Ce) helps to modify the morphology of primary and eutectic silicon particles [10], and the eutectic silicon particles are refined to a greater extent than the primary silicon particles [11–13]. Literature survey did not reveal any systematic study on the influence of semi-solid processing by electromagnetic stirring (EMS) coupled with cerium oxide addition on the microstructure and mechanical properties of hypereutectic Al–Si alloys [14–16]. Therefore, in this investigation, attempts were made to study the effect of cerium addition and electromagnetic stirring on the microstructure and mechanical properties of hypereutectic Al–Si alloys.

P. Kaur · D. K. Dwivedi (✉) · P. M. Pathak
Mechanical and Industrial Engineering Department, I.I.T., Roorkee, Uttarakhand 247667, India
e-mail: dkd04fme@iitr.ernet.in

2 Experimental procedure

2.1 Development of casting

The chemical composition of hypereutectic Al–Si alloy used in present work is shown in Table 1. The hypereutectic Al–Si alloy was produced by melting ingot of 99.9% pure Al with Al–50%Si, Al–10%Mg, Al–50%Cu and Al–30%Ni master alloys and Fe powder in an induction furnace (Table 1). The chemical composition was measured by electron dispersive spectroscopy by taking at least 10 points on each specimen. This alloy was modified by adding CeO_2 (0.2 wt.%) in the form of a powder in molten alloy. The molten alloy with CeO_2 was heated at 850ºC for 30 min to homogenise the composition and was then treated with cover flux (SARU COVER A-1F) and degasser (SARU DEGASSER D-108) for removing impurities from the melt, before pouring into the mould.

2.2 Electromagnetic stirring

The semi-solid processing of molten slurry was carried out by using an electromagnetic stirring set-up with electric field generation of 22.5 kW rating along with a suitable ammeter and a voltmeter for the measurement of current and voltage, respectively. Schematic diagram of the set-up is shown in Fig. 1. Temperature of the molten metal during EMS was measured with a K-type Alumel chromel thermocouple and a digital temperature recorder.

The crucible with molten alloy was placed in the electromagnetic field. Stirring of the melt was carried out for 2 min in the mushy zone under a temperature range from 625°C to 645°C in a graphite crucible which was preheated to 300°C. For electromagnetic stirring, the current was increased gradually from 0 to 30 A in order to increase the strength of the electromagnetic field. After stirring, slurry was poured into sand mould at 620°C±5°C. Similarly, hypereutectic Al–Si alloy with cerium oxide modification (0.2 wt.%) was also subjected to electromagnetic stirring.

2.3 Mechanical characterizations

Brinell hardness testing (BHN) of alloy in different conditions was done by using 31.25 kg load and an indenter having 2.5 mm diameter. Three indents were taken to calculate the final hardness value. Tensile testing was done using computerised tensile testing machine (2.5 kN capacity) at 1-mm/min strain rate. The gauge diameter of tensile specimen was 6 mm and the gauge length was 30 mm according to the ASTM E8 standard [17]. For all alloy compositions and conditions, each test was repeated thrice and the average values were used for study purpose on tensile testing machine [Tinius Olsen (S-series) H-25K-S, UK]. Yield strength was found the same as the ultimate tensile strength in case of hypereutectic Al–Si alloys due to their brittle nature as reported in literature [18].

Table 1 Composition of hypereutectic Al–Si alloy

Composition	Si	Cu	Mg	Fe	Ni	Al
Hypereutectic Al–Si alloy	16%	5%	0.5%	0.5%	0.1%	Balance

2.4 Metallurgical characterization

The standard metallographic procedure was used for preparing the samples for microscopy and the microstructures were taken with the help of an optical microscope. Polished samples were etched with the Keller reagent. Image analysing software namely Image J was used for image analysis of micrographs of alloys under different conditions.

The porosity (in percent) of alloys was measured at a magnification of ×50 by point counting method according to ASTM standards [19]. In this method, a grid (having grid points N_G) is used to find the fraction of specific microconstituent (porosity). The number of porous points that lie on the grid point is taken as one (N_1), whereas the porous points lying on the grid boundary are taken as half (N_2). The ratio of the total number of porous points ($N_P=N_1+N_2$) and the number of grid points (N_G) is the porosity percentage ($N_P\times 100/N_G$). Eleven different areas of the each alloy were used for average porosity and the same has been reported.

3 Results and discussion

3.1 Microstructure of alloy

The microstructures of hypereutectic Al–Si alloy in as cast, EMS cast and that subjected to both CeO_2 modification and EMS cast conditions are shown in Fig. 2a–d. The microstructure of hypereutectic Al–Si alloy in as cast condition shows large-sized PSPs and long β-intermetallic Al–Fe–Si particles in the matrix of eutectic mixture (Fig. 2a). Some copper–nickel-rich intermetallics were also observed in the matrix. Furthermore, the image analysis of the micrograph exhibited the average size of PSP and β-intermetallics as 152±9 and 314±8 μm, respectively. The average aspect ratio of primary silicon particles was 2.11±0.14. The large size of PSPs and β-intermetallics is expected to be harmful for mechanical properties of an alloy such as strength and ductility because coarse PSPs and longer β-intermetallics facilitate easy nucleation of cracks owing to high stress concentration at the particle–matrix interface and provide easy path for fracture.

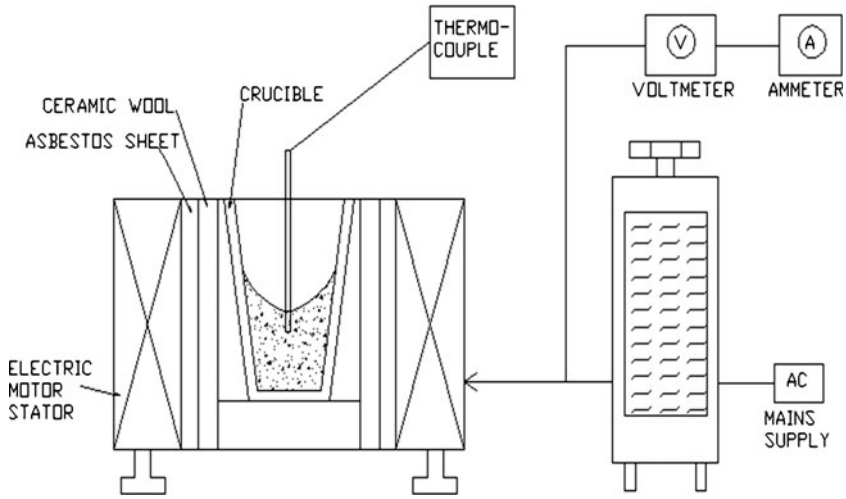

Fig. 1 Schematic diagram of electromagnetic stirring set-up

The microstructure of the alloy subjected to electromagnetic stirring is shown in Fig. 2b. It can be observed that EMS has reduced the size of PSPs and β-phase particles. Image analysis of the micrographs showed that average size of PSPs has reduced from 152±9 to 120±6 μm and the average length of β-intermetallics has reduced from 314±8 to 234±6 μm. Further image analysis of micrographs also showed that electromagnetic stirring has decreased the average aspect ratio from 2.11±0.14 to 1.849±0.11. Moreover, electromagnetic stirring has improved the distribution of PSPs, eutectic silicon and intermetallic compounds of copper–nickel. These structural modifications primarily occur due to the fragmentation of primary silicon particles and β-intermetallics owing to turbulence created in the alloy slurry (mushy zone) subjected to electromagnetic stirring during solidification. The extent of fragmentation during EMS increases due to further collision of fragmented particles during EMS process and are beneficial for the refinement of structure [12].

The microstructure of CeO_2-modified alloy in as cast condition is shown in Fig. 2c. It can be observed that coarse polyhedral shape primary silicon particles have been reduced significantly in CeO_2-modified alloy without EMS.

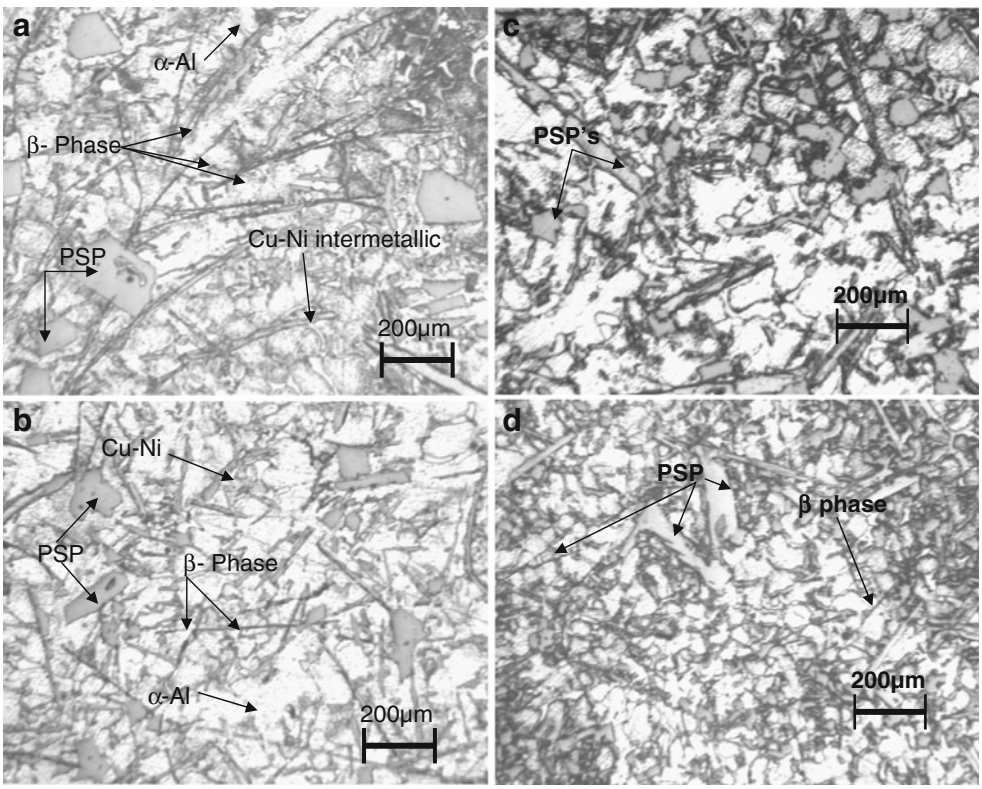

Fig. 2 Optical micrographs of hypereutectic Al–Si alloy in **a** as cast, **b** EMS cast, **c** CeO_2-modified as cast and **d** CeO_2-modified and EMS cast

The image analysis of the micrograph revealed that CeO_2 modification of alloy in as cast condition reduced: (a) the average size of primary silicon particles from 152±9 to 98±5 μm, (b) the average aspect ratio of primary silicon particles from 2.11±0.14 to 1.35±0.08 and (c) the average length of β-intermetallic particles from 314±8 to 221±4 μm. EMS processing of CeO_2-modified alloy further reduced: (a) the average size of primary silicon particles from 98±5 to 76±4 μm, (b) the average aspect ratio of primary silicon particles from 1.35±0.08 to 1.16±0.08 and (c) the average length of β-intermetallic particles from 221±4 to 203±5 μm. X-ray diffraction (XRD) analysis revealed that CeO_2 got partly absorbed and partly survived in the melt as evident from the presence of CeO_2- and Ce-based compounds in the alloy (Fig. 3b).

It was found that porosity (in percent) for unmodified and as cast hypereutectic Al–Si alloy was 5.87±0.23 and that of EMS cast was 5.29±0.19. Similarly, the value of porosity (in percent) for CeO_2-modified alloy in as cast condition was measured as 4.55±0.16 and that of EMS cast was 3.88±0.14. EMS helped in reducing the porosity (in percent) although marginally.

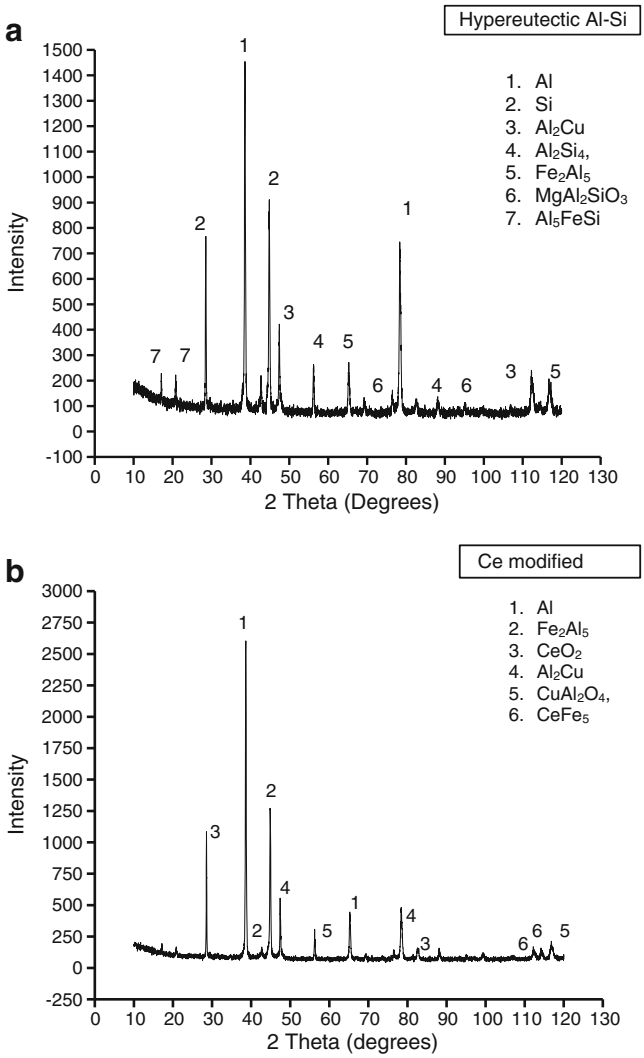

Fig. 3 X-ray diffraction pattern of alloy in **a** unmodified and **b** CeO_2-modified condition showing different phases present in the alloy

It has been reported that Ce addition refines and modifies the microstructure of hypereutectic Al–Si alloys by changing the morphology of eutectic silicon from plate-like acicular structure to fibrous one [10, 11]. To act as nucleation site for Si (like AlP), the RE compound should solidify at temperature higher than Si besides having crystal structure similar to that of Si. However, Ce has been reported to form AlCe compound having an orthorhombic crystal structure and a melting point of 845ºC. Although Ce compound solidifies at a temperature higher than Si, but due to mismatching of the crystal structure, CeO_2 may not act as nucleants for the refinement for primary Si particles [16]. Thus, the mechanism of the refinement of primary silicon as well as eutectic silicon by RE cannot be attributed to the heterogeneous nucleation. The mechanism of refinement of primary silicon particles in hypereutectic Al–Si alloy treated with CeO_2 can be related to the reduction in nucleation temperature of silicon and the modification of both solid–liquid interfacial energy and the surface energy of solid silicon [4]. Moreover, the improved chemical composition in the molten alloy and fragmentation of solidifying constituents due to electromagnetic stirring in the presence of CeO_2 can be attributed to the refinement of eutectic and primary silicon particles.

X-ray diffraction analysis of the unmodified hypereutectic Al–Si alloy revealed the phases like Al, Si, Al_2Si_4, Al_2Cu, Fe_2A_5, $MgAl_2SiO_3$ and Al_5FeSi, while the XRD study of CeO_2-modified alloy showed the presence of Al, Fe_2Al_5, CeO_2, Al_2Cu, $CuAl_2O_4$ and $CeFe_5$ phases. The presence of CeO_2 and $CeFe_5$ indicated successful addition of CeO_2 in the alloy (Fig. 3a, b).

3.2 Mechanical properties

The effect of electromagnetic stirring and CeO_2 addition on hardness and tensile properties is shown in Table 2. It can be observed that EMS of unmodified and CeO_2-modified hypereutectic Al–Si alloy increases the hardness from 99±1.8 to 118±1.0 BHN and 120±1.3 to 123±1.5 BHN, respectively. An increase in the hardness of CeO_2-modified alloy after electromagnetic stirring can be attributed to the improved distribution and refinement of primary silicon particles. Increase in hardness of alloy subjected to electromagnetic stirring is marginal.

The tensile properties of unmodified and CeO_2-modified hypereutectic Al–Si alloy in as cast and EMS cast condition are shown in Table 2. Tensile strength of the hypereutectic

Table 2 Effect of stirring current on tensile strength

S. no.	Alloy condition	Hardness (BHN)	Ultimate tensile strength (MPa)	Tensile yield strength (MPa)	% Elongation
1	Hypereutectic Al–Si alloy + no stirring	99±1.8	107±3.3	107±3.3	2.2±0.03
2	Hypereutectic Al–Si alloy + EMS	118±1.0	119±4.2	119±4.2	2.4±0.06
3	Hypereutectic Al–Si alloy + CeO_2 + no stirring	120±1.3	128±4.4	128±4.4	3.4±0.08
4	Hypereutectic Al–Si alloy + CeO_2 + EMS	123±1.5	139±5.2	139±5.2	4.5±0.11

BHN Brinell hardness testing, *EMS* electromagnetic stirring

Al–Si alloy in the present study is lower [18], and this can be attributed to slight difference in composition and porosity which arise in the casting. As discussed in Section 2.3, that ultimate tensile strength and yield strength for the present alloy are the same as reported in literature for A390 (similar to the present alloy except the inclusion of Zn, Mn and Ti). The results of the tensile test conducted on alloys in different conditions in the present study are given in Table 2. Primary reasons for lower tensile properties are: (1) difference in composition of the present alloy with A390 and (2) shape and size of structural features such as large average size of primary silicon particles and longer length of β-intermetallics as they provide easy path for nucleation and growth of cracks which are detrimental for the tensile properties as in our case (Figs. 2a and 3) porosity may also be another important reason for lower tensile properties again due to availability of easy path of fracture as pores cannot resist stress. It can be observed that in general, the electromagnetic stirring and CeO_2 modification improve the tensile properties. This improvement in tensile properties can be attributed to the refinement of primary silicon particles and reduction in average size of PSPs and beta-intermetallics. A reduction in size of the hard second phase particles in comparatively soft matrix is known to increase the stress required for nucleation and growth of cracks needed for fracture. Furthermore, the presence of coarse polyhedral-shaped primary silicon particles in as cast condition of alloy causes brittle fracture and limited ductility as evident from SEM fractograph of the alloy (Fig. 4a). The flat and smooth fracture surfaces in fractograph represents the fracture of primary silicon particles and bright cleavage facets correspond to the fracture of eutectic region in alloy. Tensile fracture surface of CeO_2-modified alloy also exhibited similar kind of features (Fig. 4b).

4 Conclusions

- The EMS processing of hypereutectic Al–Si alloy under study refined the PSPs and β-intermetallics and improved the mechanical properties.
- The modification of hypereutectic Al–Si alloys with CeO_2 addition also refined the microstructure and improved the mechanical properties significantly.
- The combined effect of EMS and CeO_2 addition resulted in further refinement of primary silicon particles and β-intermetallics and improved the mechanical properties.
- Porosity reduced the tensile strength of the alloys and EMS helped in reducing the porosity although marginally and improved the tensile strength.

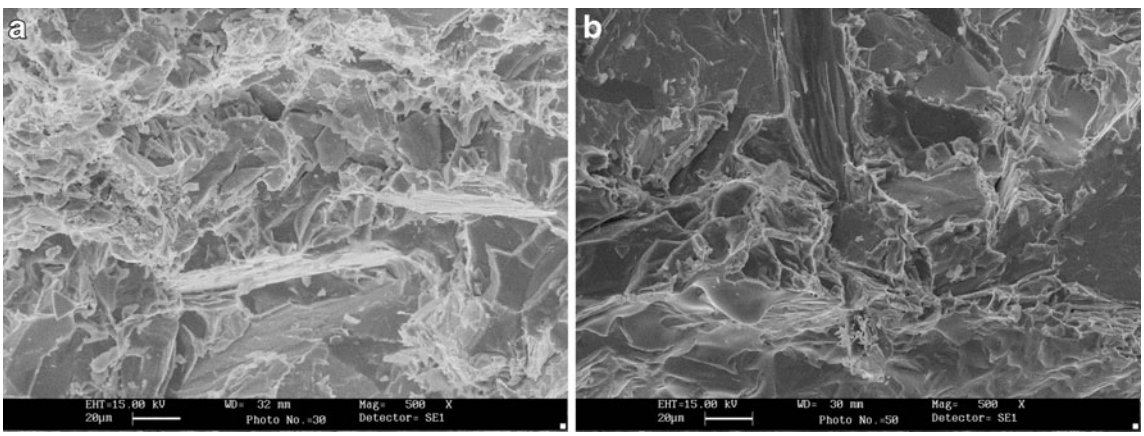

Fig. 4 SEM micrographs of tensile fracture surfaces of alloy in **a** as cast and **b** CeO_2-modified condition

Acknowledgements The authors are grateful to DST and GOI for funding this research project under project grant no. DST/INT/MEX/RPO-07/2008.

References

1. Fan Z (2002) Semisolid metal processing. Int Mater Rev 47:1–37
2. Sung CL, Eui PY, Jung SK (1997) The effect of electromagnetic stirring on the microstructure of Al-7 wt% Si alloy. J Mater Sci Lett 16:104–109
3. Atkinson H (2007) Current status of semi-solid processing of metallic materials. Springer, Paris, pp 81–98, Adv In Mater forming
4. Chong C, Zhong L, Bo R, Ming W, Yong W, Zhi L (2007) Influences of complex modification of P and RE on microstructure and mechanical properties of hypereutectic Al-20Si alloy. Trans Nonferrous Met Soc China 17:301–306
5. Henghua Z, Haili D, Guangjie S, Luoping X, Junlin Y, Biao Y (2006) Modification mechanism of cerium on the Al-18Si alloy. Rare Met 25:11–15
6. Zhao YG, Qin QD, Zhou W, Liang YH (2005) Microstructure of the Ce modified in situ Mg_2Si/Al-Si-Cu composite. J Alloys Compd 389:1–4
7. Sebaie OEI, Samuel AM, Samuel FH, Doty HW (2008) The effects of misch metal, cooling rate and heat treatment on the eutectic Si particle characteristics of A319.1, A356.2 and A413.1 Al-Si casting alloys. Mater Sci Eng A 480:342–355
8. Daud AR, Wong KMC (2004) The effect of cerium additions on dent resistance of Al-0.5Mg-1.2Si-0.25Fe alloy for automotive body sheets. Mater Lett 58:2545–2547
9. Yizhen L, Qudong W, Xiaoqin Z, Wenjiang D, Chunquan Z, Yanping Z (2000) Effects of rare earths of the microstructure, properties and fracture behavior of Mg-Al alloys. Mater Sci Eng A 278:66–76
10. Xiao DH, Wang JN, Ding DY, Yang HL (2003) Effect of rare earth Ce addition on the microstructure and mechanical properties of an Al-Cu-Mg-Ag alloy. J Alloys and Compds 352:84–88
11. Hasseinifar M (2009) Physical metallurgy and thermodynamics of aluminium alloys containing cerium and lanthanum, PhD thesis, McMaster University, Canada
12. Nafisi S, Emadi D, Shehata MT, Ghomashchi R (2006) Effects of electromagnetic stirring and superheat on the microstructural characteristics of Al-Si-Fe alloy. Mater Sci Eng A 432:71–83
13. Kang CG, Bae JW, Kim BM (2007) The grain size control of A356 aluminium alloy by horizontal electromagnetic stirring for rheology. J Mater Process Technol 187–188:344–348
14. Joonyeon C, Inge M, Chongsool C (1998) Refinement of cast microstructure of hypereutectic Al-Si alloys through the addition of rare earth metals. J Mater Sci 33:5015–5023
15. Mondolfo LF (1976) Aluminium alloys: structure and properties. Butterworth, London
16. Anasyida AS, Daud AR, Ghazali MJ (2010) Dry sliding wear behavior of Al-12Si-Mg alloy with cerium addition. Mater Des 313:65–374
17. ASTM (2008) ASTM standards: E8/E8M-08 standard test methods for tension testing of metallic materials. ASTM International, West Conshohocken
18. ASM (1990) ASM handbook: properties and selection: nonferrous alloys and special purpose materials, vol 2. ASM International, West Conshohocken
19. ASTM (2005) ASTM standards: E 562–05e1 standard test method for determining volume fraction by systematic manual point count. ASTM International, West Conshohocken